Preprints of the 19th World Congress
The International Federation of Automatic Control
Cape Town, South Africa. August 24-29, 2014

Probabilistic Trajectory Prediction in Intelligent Driving ⋆

Xiaoxin Fu * **Yongheng Jiang** ** **Geng Lu** ***
Jingchun Wang **** **Dexian Huang** † **Danya Yao** ‡

* *Department of Automation, Tsinghua University, Beijing, China (e-mail: fuxx10@mails.tsinghua.edu.cn)*
** *Department of Automation, Tsinghua University, Beijing, China (e-mail: jiangyh@tsinghua.edu.cn)*
*** *Department of Automation, Tsinghua University, Beijing, China (e-mail: lug@mail.tsinghua.edu.cn)*
**** *Department of Automation, Tsinghua University, Beijing, China (e-mail: wang-jc@tsinghua.edu.cn)*
† *Department of Automation, Tsinghua University, Beijing, China (e-mail: huangdx@tsinghua.edu.cn)*
‡ *Department of Automation, Tsinghua University, Beijing, China (e-mail: yaody@tsinghua.edu.cn)*

Abstract: For intelligent vehicles, trajectory prediction for their surrounding traffic participants is the basis of their ego trajectory planning. Since there exist various uncertain factors that influence the driving processes, the participants' future trajectories are uncertain either. Unique deterministic prediction results provided by traditional methods do not involve the probability information of different trajectories, and thus are insufficient. To solve this problem, a probabilistic trajectory prediction model is proposed here, and uncertain future trajectories are designed to be described with position probability distributions at discrete moments. In the proposed model, the predicted participant's motion is decomposed into lateral and longitudinal motions which are independent with each other. Probabilistic trajectories are calculated in these two directions respectively and then are combined into complete ones. Furthermore, the model considers two driving modes(Free driving and Vehicle-following modes) in the longitudinal motion, and thus computes trajectories in different ways. Besides, we also modeled the features of different types of participants and the interaction between their trajectories. Model parameters are identified off-line based on historical trajectory data, therefore only iterative computations are needed when the model is applied on-line. The experimental results show that the proposed method has higher prediction accuracy than the traditional ones, and can meet the demands of real-time applications.

Keywords: Trajectory prediction, Intelligent vehicles, Markov chains, Off-line identification, Trajectory planning, Driving decision-making

1. INTRODUCTION

Intelligent vehicles have become a worldwide research focus, because of their benefits to transportation and our daily lives. On busy urban roads, the driving environment is changing all the time. Before planning their ego trajectories, intelligent vehicles need to estimate their surrounding traffic participants' future motion and find the feasible moving region firstly. Therefore, trajectory prediction for participants constitutes the basis of trajectory planning, which is critical to achieving intelligent driving. Along with the development of intelligent vehicles in the past 30 years, trajectory prediction also attracts attentions from researchers all over the world.

Essentially, for intelligent vehicles, the goal of trajectory prediction is to recognize the future trends of the relative motion between their surrounding obstacles and themselves. Some researchers directly choose to compute some predefined safety evaluation indicators, such as TTC(Time To Collision, Labayrade et al. (2005)) and TTB(Time To Brake, Keller et al. (2011)), to estimate the collision possibility. Instead of computing concrete trajectories, they simply assume that all concerned objects will move at constant velocities. Without considering the complexity of the real world, these methods are computationally simple, but may result in collision risks and low traffic efficiency. Some other methods(Jula et al. (2000); Ferguson et al. (2008)) apply simplified kinematic models combined with road geometry to forecast the concerned participants' behaviors. These methods assume that the objects' velocities are invariant and their motion is independent of each other. As a result, their autonomy and uncertainties are

⋆ This work was supported in part by the National Natural Science Foundation of China under the Grants 61203071.

ignored, and the prediction error can accumulate quickly over time. Therefore, the application of these methods in multiple-vehicle situations is restricted. Some researchers apply filter techniques(e.g. Kalman Filter) to estimate vehicles' future motion states. Although the measurement and process noises are considered, the possibilities of different trajectory executions are still not involved, because the prediction results are deterministic. Since the future acceleration is unknown, either short-term prediction(Kammel et al. (2008)) with frequent updates of sensor measurements, or long-term prediction(Glaser et al. (2010)) with constant acceleration assumptions were done. As traditional methods only compute single trajectories, Monte Carlo experiments(Broadhurst et al. (2005); Danielsson et al. (2007)) are introduced into prediction. These new methods sample stochastically in the state space and input space, and combine variable initial conditions with various driving behaviors to simulate multiple future trajectories. However, this consumes a large amount of computing resources and may neglect critical dangerous situations. Probability distributions(PDs) [1] of motion states are firstly introduced by Althoff et al. (2009) to describe the possibilities of performing different trajectories. The stochastic reachable sets decide all possible states that the trajectories can evolve into, thus are applied to compute the transition probabilities between motion states. Then the predicted objects' motion state PDs become computable. However, though their prediction results are given, the prediction error of their method is not discussed.

In this paper, based on the idea of probabilistic trajectories proposed in Althoff et al. (2009), a novel probabilistic trajectory prediction method is proposed. Not only the uncertainties in driving decisions are modeled, but also driving habits and behavioral characteristics of different types of objects are considered. Besides, the interaction between traffic participants is included in the proposed model as well. With the acceleration PDs generated offline, probabilistic trajectories can be calculated. The rest of this paper is organized as follows. In section 2, the challenges encountered in trajectory prediction problems are illustrated, and the basic prediction idea is introduced. Section 3 presents the flowchart, model structure, and computing method of probabilistic trajectory prediction. Section 4 introduces the prediction of longitudinal trajectories in two driving modes. In section 5, a numerical example is used to illustrate the prediction result. Then the performance of our proposed model is demonstrated by comparing with a traditional model. Finally, in section 6, the paper is concluded and future work is discussed.

2. PROBLEM STATEMENT

The traffic participants discussed in this paper refer to those common vehicles driving on urban roads. Since the information about other drivers' decisions is usually unavailable, it is not easy to predict their vehicle trajectories. Besides, drivers' control on vehicles can be influenced by multiple human factors, which results in uncertain trajectories and makes the prediction even harder. Firstly, because of the limitation of driving abilities, there must exist some error between the actually executed trajectories and the expected ones. For instance, it is impractical for vehicles to drive along the centerlines of lanes absolutely precisely. Secondly, drivers' decisions can be affected by various physical and mental factors(e.g. age, fatigue, emotion, etc). This may cause uncertainties in vehicle trajectories. Lastly, drivers of different types of vehicles have different driving habits, which determines that their vehicle trajectories show corresponding features. If the difference is not considered, unnegligible deviations may be caused in trajectory prediction. However, even so, vehicle trajectories are not irregular stochastic motion. Since the driving decisions are made based on human's common daily experience, driving behaviors should statistically obey specific distributions. For example, if a vehicle's space headway decreases to the danger threshold, it is more likely to decelerate rather than accelerate.

Traditional prediction methods simply assume that vehicle velocities are constant, thus can only provide single possible trajectories. These methods do not utilize the probability information of driving decisions, therefore can not compute the possibilities of different trajectories. However, for an intelligent vehicle, its surrounding traffic participants are all dynamic obstacles. In order to acquire an accurate evaluation of its driving scenario, it is essential to consider the possibilities of obstacles' different trajectories. Note that, vehicle positions are the integral of their accelerations, thus we can make use of the acceleration PDs to quantify and compute uncertain trajectories. In this paper, acceleration PDs are identified based on historical trajectory data and combined with kinematic equations to compute probabilistic trajectories. To facilitate the estimation of vehicles' relative motion, probabilistic trajectories are designed to be the predicted objects' position PDs at different time points.(The velocity information has been included in position PDs at adjacent time points.) To simplify the prediction, here vehicle motion is decomposed into lateral and longitudinal motions, which represent the motions perpendicular to and along the lane centerline, respectively. Through computing one-dimensional position PDs in these two directions, the original two-dimensional PDs can be acquired.

The proposed prediction model hypothesize that:

Hypothesis 1. The concerned vehicles do not change lanes. The predicted objects keep driving in single lanes and lane changing behaviors are not considered here.

Hypothesis 2. The position PDs in lateral and longitudinal directions are independent of each other. In the lateral direction, the vehicle is controlled for tracking centerlines as precisely as possible. But the control of the longitudinal motion focuses on the vehicle's velocity, which mainly depends on its absolute and relative motion states. Therefore, driving processes in these two directions are distinctively different. Through assuming the independence between their position PDs, the calculation of a two-dimensional position PD can be simplified as the calculation of two one-dimensional PDs.

Hypothesis 3. Those vehicles whose preceding vehicle information is unavailable, are assumed to move at constant speeds. For the objects that are located next to the front boundary of the prediction space range, their preceding vehicles' motion states are unmeasurable. Then

[1] In the rest of this paper, "probability distribution" is all abbreviated as PD.

their future trajectories cannot be predicted. Therefore, these vehicles' velocities(measured when the prediction starts) are considered as unchanged. Since their impacts on intelligent vehicles are limited, the above simplification is acceptable.

3. PREDICTION MODEL

This section introduces the implementation of probabilistic trajectory prediction. Section 3.1 presents its flowchart and model structure, while in section 3.2, the representation and calculation of probabilistic trajectories are discussed.

3.1 Model Framework

In the proposed model, the predicted traffic participants include all the vehicles that are located in a certain space range of the ego vehicle. Probabilistic trajectory prediction is a process of rolling computation, as is shown in Fig. 1. In the beginning of every working cycle T_{drive}, initial motion states of the concerned vehicles are acquired. Then their future trajectories in prediction time horizon $(0, T_{pre})$ are calculated. When the prediction is finished, the model will wait until the current working cycle is over. After that, the next cycle starts and the above steps are repeated. For safety, T_{pre} is chosen larger than T_{drive} to ensure that prediction results cover all time.

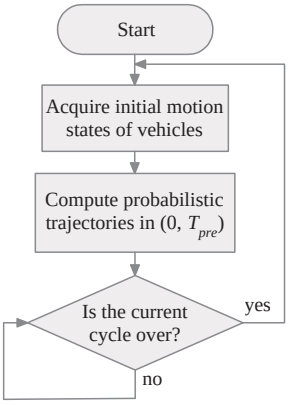

Fig. 1. The flowchart of probabilistic trajectory prediction

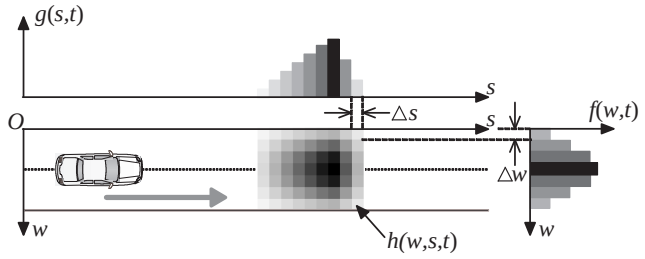

Fig. 2. The combination of lateral and longitudinal position PDs

The vehicles' probabilistic trajectories are represented by two-dimensional discrete PDs of their positions in the road plane at discrete time points, i.e. $h(w, s, t)$ where w and s are the lateral and longitudinal positions, $t(0 \leq t \leq T_{pre})$ represents time. According to *Hypothesis 2*, $h(w, s, t)$ can be calculated by multiplying the lateral position PD $f(w, t)$ and longitudinal position PD $g(s, t)$. Fig. 2 shows the combination of $f(w, t)$ and $g(s, t)$. The two-dimensional PD $h(w, s, t)$ is expressed as a series of squares with different gray values. A darker square means a higher discrete probability in $h(w, s, t)$.

The model parameters used for computing trajectories are identified based on a data set of historical trajectories. Since they are all discrete PDs of different variables, here we name them as PD parameters. Note that the vehicles can be classified into 3 categories: motorcycles, automobiles, and trucks. Obviously, their sizes and masses vary greatly between categories, and their drivers have distinct driving habits and behavioral features. Consequently, 3 types of vehicles use 3 groups of PD parameters. The PD parameters used in the lateral motion model are vehicles' lateral position PDs, which are identified by computing corresponding histograms off-line. The PD parameters used in the longitudinal motion model are, vehicles' acceleration conditional PDs given different driving modes and motion states. Similarly, these PD parameters are identified by computing acceleration histograms under the same conditions.

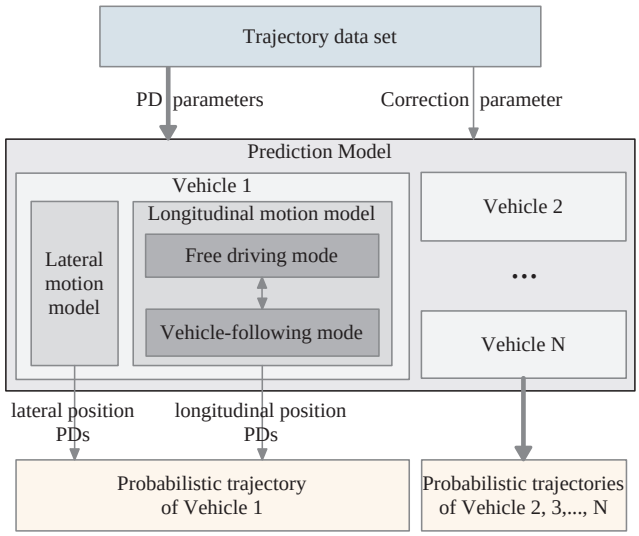

Fig. 3. The structure of probabilistic trajectory prediction model

In the model structure shown in Fig. 3, each predicted vehicle's probabilistic trajectory is determined by its lateral and longitudinal position PDs. The lateral PDs are given by the lateral motion model parameters. The longitudinal motion switches between two driving modes(Free driving and Vehicle-following modes), and thus the longitudinal PDs are computed with the mode-relied model parameters.

In this model, vehicles' continuous longitudinal motion is discretized into transitions between their discrete motion states. Inevitably, state discretization will introduce calculation error. As a result, position PDs are shifted. Therefore, θ is introduced as the correction parameter to adjust original results. Through translating biased position PDs, errors can be minimized. Fig. 4 illustrates the correction process of the longitudinal position PD $g(s, t)$. Given the start position of longitudinal motion as s_0 and the discrete position with the largest probability in $g(s, t)$ as s_m, the

translating quantity is calculated by multiplying θ with the driving distance corresponding to s_m. The corrected PD $g'(s,t)$ can be written as

$$g'(s,t) = g(s - \theta \cdot (s_m - s_0), t). \quad (1)$$

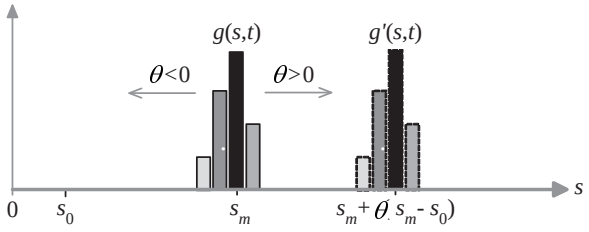

Fig. 4. The correction of the longitudinal position PD

In order to evaluate the prediction accuracy of the proposed model, we define e_{lat} and e_{lon} as the largest error of a single lateral and longitudinal position predictions, repectively. $e_{lat}(e_{lon})$ is calculated as the maximum of the errors between expectations of lateral(longitudinal) PDs and actual values at all time points. Additionally, the average value of e_{lat} and e_{lon} is defined as the average prediction error of multiple lateral and longitudinal predictions, respectively, i.e. ERR_{lat} and ERR_{lon}. Then the optimal correction parameter θ_{opt} should be chosen to minimize ERR_{lon} of the corrected PDs, i.e.

$$\theta_{opt} = \arg\min_{\theta} \mathrm{ERR}_{lon}. \quad (2)$$

3.2 Prediction of Probabilistic Trajectories

In this paper, the predicted vehicles are all treated as mass points when we compute their future trajectories. The prediction time horizon T_{pre} is divided into R time periods with length $T = T_{pre}/R$. Vehicles are thought to move at constant accelerations in each period. Since the vehicle trajectories are decomposed into lateral and longitudinal motions, the road is accordingly discretized into intervals of equal sizes along these two directions(see Fig. 2), i.e.

$$\begin{aligned} W_l &\triangleq (w_l - \Delta w, w_l), w_l = w_0 + l \cdot \Delta w, \\ S_i &\triangleq (s_i - \Delta s, s_i), s_i = s_0 + i \cdot \Delta s, \\ l &\in \{1,2,...,L\}, i \in \{1,2,...,I\}, \end{aligned} \quad (3)$$

where $W_l(S_i)$ represents the lth lateral(ith longitudinal) interval, $w_0(s_0)$ is the lateral(longitudinal) start position, $\Delta w(\Delta s)$ is the length of lateral(longitudinal) intervals, $w_l(s_i)$ is the discrete position corresponding to $W_l(S_i)$.

The discrete PD $F^{(r)}_{\alpha lat}(F^{(r)}_{\alpha lon})$ of a vehicle α's lateral(longitudinal) position $w^{(r)}_{\alpha}(s^{(r)}_{\alpha})$ at $t = rT(r \in \{1,2,...,R\})$ is defined as

$$\begin{aligned} F^{(r)}_{\alpha lat} &\triangleq \{p^{(r)}_{\alpha l}, l \in \{1,2,...,L\}\}, p^{(r)}_{\alpha l} = P(w^{(r)}_{\alpha} \in W_l), \\ F^{(r)}_{\alpha lon} &\triangleq \{p^{(r)}_{\alpha i}, i \in \{1,2,...,I\}\}, p^{(r)}_{\alpha i} = P(s^{(r)}_{\alpha} \in S_i). \end{aligned} \quad (4)$$

With the independence between $F^{(r)}_{\alpha lat}$ and $F^{(r)}_{\alpha lon}$, the probability $f^{(r)}_{\alpha li}$ that α is located in the rectangle region $W_l \cap S_i$ can be calculated as $f^{(r)}_{\alpha li} = p^{(r)}_{\alpha l} \cdot p^{(r)}_{\alpha i}$. Then, the two-dimensional discrete PD of α's position in the road plane at $t = rT$ can be described as $F^{(r)}_{\alpha} = \{f^{(r)}_{\alpha li}, l \in \{1,2,...,L\}, i \in \{1,2,...,I\}\}$. In this way, the calculation of α's probabilistic trajectory is transformed into the calculation of its lateral and longitudinal position PDs at different time points, i.e. $F^{(r)}_{\alpha lat}$ and $F^{(r)}_{\alpha lon}$($r \in \{1,2,...,R\}$). The rest of this section will illustrate the computation of $F^{(r)}_{\alpha lat}$ and $F^{(r)}_{\alpha lon}$.

Lateral Motion Model A vehicle's lateral motion represents its decomposed trajectory perpendicular to the road centerline. In (4), $p^{(r)}_{\alpha l}$ denotes the probability that α's lateral position at $t = rT$ is in the interval W_l, then we can define α's lateral probability vector $\mathbf{p}_{\alpha lat}(rT)$ as

$$\mathbf{p}_{\alpha lat}(rT) \triangleq \left[p^{(r)}_{\alpha 1}, \ldots, p^{(r)}_{\alpha l}, \ldots, p^{(r)}_{\alpha L}\right]^{\mathrm{T}}. \quad (5)$$

With $\mathbf{p}_{\alpha lat}((r-1)T)$, the prediction equation of the lateral motion model can be expressed as

$$\mathbf{p}_{\alpha lat}(rT) = \Phi_{\alpha lat} \cdot \mathbf{p}_{\alpha lat}((r-1)T), \quad (6)$$

where $\Phi_{\alpha lat}$ is α's lateral transition probability matrix.

From the perspective of a driver, his vehicle's lateral trajectory can be seen as a process where the lateral position keeps tracking an expected value. Therefore, the vehicle α's lateral position $w^{(r)}_{\alpha}$ can be equivalent to a sum of its expected position w_{exp} and tracking error ε, i.e. $w^{(r)}_{\alpha} = w_{exp} + \varepsilon$. Since the predicted vehicles are assumed to keep driving in single lanes(see *Hypothesis 1*), w_{exp} is a constant corresponding to the lane centerline, and ε can be seen as a random variable that obeys a time-independent PD. As a result, $\mathbf{p}_{\alpha lat}(rT)$ does not change with time, and $\Phi_{\alpha lat}$ is the identity matrix.

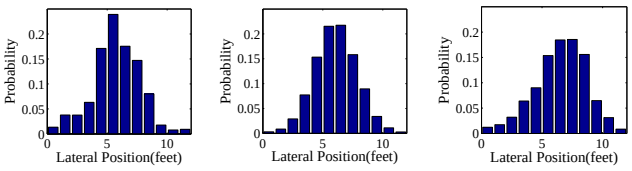

(a) Motorcycles (b) Automobiles (c) Trucks

Fig. 5. Lateral position PDs of different types of vehicles

Consequently, with the historical trajectory data, histograms of vehicles' lateral positions can be computed as the estimation of $\mathbf{p}_{\alpha lat}(rT)$, i.e. the PD parameters of the lateral motion model. Fig. 5 presents the lateral position PDs of different types of vehicles. The horizontal axis represents the vehicle's lateral position(the lane whose standard width is 3.66m(12feet) is divided into 12 intervals). The vertical axis represents the probabilities corresponding to different intervals. Usually, the motorcycles are small and narrow in size, and their driver seats are located on the centerlines of the vehicle bodies, so that it is easier for their drivers to track the expected lateral positions(see Fig. 5(a), the probability corresponding to the interval (1.52m,1.83m)((5feet,6feet)) is obviously higher than the rest). However, for automobiles and trucks in America, their sizes and widths are significantly larger, and the driver seats are transferred to the left. Note that, drivers are psychologically more sensitive to the closer obstacles.

Thus these larger vehicles may be unconsciously controlled in the near right of the lane centerline, to keep away from the obstacles in the left neighbor lane(see Fig. 5(b),5(c)). This effect is more apparent with larger vehicles, as is shown by the difference between Fig. 5(b) and Fig. 5(c).

According to the discussion above, lateral position PDs in Fig. 5 consist with our daily driving experiences. We use them to predict lateral trajectories. Since the vehicle α's lateral probability vector $\mathbf{p}_{\alpha lat}(rT)$ is constant, the lateral position PD $F_{\alpha lat}^{(r)}$ in (4) can be rewritten as

$$F_{\alpha lat} = \{p_{\alpha l}, l \in \{1, 2, ..., L\}\}. \tag{7}$$

Longitudinal Motion Model A vehicle's longitudinal motion can be seen as one-dimensional motion that aims at speed control. According to our driving experiences, a driver's operations(i.e. throttle and braking) mainly depend on his vehicle's motion state in the current moment, but are not much related to previous moments. Therefore, Markov chains are widely applied in the modeling of vehicle motion(Krumm (2008); Pentland and Liu (1999)). In this work, each predicted vehicle's longitudinal motion is also abstracted as an independent discrete Markov chain, whose system state X is consisted of the vehicle position S and velocity V. The vehicle's continuous motion state space is also discretized into rectangular cells of equal sizes. Each cell represents a discrete state $X_m(m \in \{1, 2, ..., M\}, M = I \cdot J)$, which corresponds to the combination of a position interval $S_i(i \in \{1, 2, ..., I\})$ and a velocity interval $V_j(j \in \{1, 2, ..., J\})$, i.e.

$$\begin{array}{c} X_m \triangleq (S_i, V_j), m = J(i-1) + j, \\ S_i \triangleq (s_i - \Delta s, s_i), s_i = s_0 + i \cdot \Delta s, \\ V_j \triangleq (v_j - \Delta v, v_j), v_j = v_0 + j \cdot \Delta v, \end{array} \tag{8}$$

where S_i,s_0,Δs,s_i are the same as defined in (3), V_j represents the jth velocity interval, v_0 is the minimum velocity considered in this model, Δv is the length of velocity intervals, v_j is the discrete velocity corresponding to V_j.

Given the vehicle α's longitudinal position and velocity at $t = rT$ as $s_\alpha^{(r)}$ and $v_\alpha^{(r)}$, the probability $p_{\alpha m}^{(r)}$ that α is in the state X_m can be described as

$$p_{\alpha m}^{(r)} = P(s_\alpha^{(r)} \in S_i, v_\alpha^{(r)} \in V_j). \tag{9}$$

Then, we can define α's longitudinal probability vector $\mathbf{p}_{\alpha lon}(rT)$ as

$$\mathbf{p}_{\alpha lon}(rT) \triangleq \left[p_{\alpha 1}^{(r)}, \ldots, p_{\alpha m}^{(r)}, \ldots, p_{\alpha M}^{(r)}\right]^{\mathrm{T}}. \tag{10}$$

Similar to (6), the prediction equation of the longitudinal motion model can be expressed as

$$\mathbf{p}_{\alpha lon}(rT) = \Phi_{\alpha lon} \cdot \mathbf{p}_{\alpha lon}((r-1)T), \tag{11}$$

where $\Phi_{\alpha lon} = [\phi_{nm}]_{M \times M}$ is α's longitudinal transition probability matrix, ϕ_{nm} is the element located in the nth row and mth column of $\Phi_{\alpha lon}$.

Obviously, $\Phi_{\alpha lon}$ depends on α's acceleration PD at the same time point. Since the longitudinal motion model considers two different driving modes(Free driving mode and Vehicle-following mode), α's constant acceleration $a_\alpha^{(r)}$ in the time interval $((r-1)T, rT)$ should obey a discrete conditional PD $F_{\alpha a}^{(r)}$ given its driving mode and motion state at the start of $((r-1)T, rT)$. If K possible acceleration values$\{a_1, a_2, ..., a_K\}$ are considered here, $F_{\alpha a}^{(r)}$ can be defined as

$$\begin{array}{c} F_{\alpha a}^{(r)} \triangleq \left\{q_{\alpha k}^{(r)}, k \in \{1, 2, ..., K\}\right\}, \\ q_{\alpha k}^{(r)} = P(a_\alpha^{(r)} = a_k | \mathrm{DM}_\alpha^{(r-1)}, \mathrm{MS}_\alpha^{(r-1)}), \end{array} \tag{12}$$

where $\mathrm{DM}_\alpha^{(r-1)}$ and $\mathrm{MS}_\alpha^{(r-1)}$ are α's driving mode and motion state at $t = (r-1)T$. $\mathrm{DM}_\alpha^{(r-1)}$ can be *Free driving* or *Vehicle-following*, and $\mathrm{MS}_\alpha^{(r-1)}$ represents different motion state variables in different driving modes.

According to the memoryless property of Markov chains, the next state depends only on the current state and not on preceding states. If the vehicle α is currently in the state X_m with the longitudinal position s_i and velocity v_j, then after the acceleration a_k takes effect for time T, its position $s_{end}(m,k)$ and velocity $v_{end}(m,k)$ in the next moment can be calculated as

$$\begin{array}{c} s_{end}(m,k) = s_i + v_j T + a_k T^2/2, \\ v_{end}(m,k) = v_j + a_k T. \end{array} \tag{13}$$

Given that $s_{end}(m,k) \in S_{\widetilde{i}}$ and $v_{end}(m,k) \in V_{\widetilde{j}}$, with (12)(13), ϕ_{nm} in $\Phi_{\alpha lon}$ is given by

$$\phi_{nm} = \sum_k r(m,k,n) \cdot q_{\alpha k}^{(r)}, \tag{14}$$

where

$$r(m,k,n) = \begin{cases} 1 & \text{if } n = J(\widetilde{i}-1) + \widetilde{j} \\ 0 & \text{else} \end{cases}. \tag{15}$$

Furthermore, through computing with (11)(14) repeatedly, α's longitudinal probability vector at all discrete time points $\mathbf{p}_{\alpha lon}(T), \mathbf{p}_{\alpha lon}(2T), ..., \mathbf{p}_{\alpha lon}(RT)$ can be acquired. Consequently, α's longitudinal position PDs $F_{\alpha lon}^{(r)}(r \in 1, 2, ..., R)$ in (4) can be calculated as

$$\begin{array}{c} F_{\alpha lon}^{(r)} = \{p_{\alpha i}^{(r)}, i \in 1, 2, ..., I\}, \\ p_{\alpha i}^{(r)} = \sum_j P(s_\alpha^{(r)} \in S_i, v_\alpha^{(r)} \in V_j). \end{array} \tag{16}$$

Since the acceleration PDs given different conditions determine the value of $\Phi_{\alpha lon}$, they are chosen as the PD parameters of the longitudinal motion model. Similarly, through computing acceleration histograms under different conditions, we can obtain a series of empirical distributions as the approximation of conditional PDs. In section 4, the acquisition of acceleration PDs $F_{\alpha a}^{(r)}$ in two driving modes will be presented.

4. DRIVING MODES IN LONGITUDINAL MOTION MODEL

In the proposed longitudinal motion model, $F_{\alpha a}^{(r)}$ is the vehicle α's acceleration conditional PD given $\mathrm{DM}_\alpha^{(r-1)}$ and $\mathrm{MS}_\alpha^{(r-1)}$, which determines the transition probabilities between α's motion states. Section 4.1 and 4.2 will discuss the meaning and calculation of $F_{\alpha a}^{(r)}$ in Free driving mode and Vehicle-following mode, respectively.

4.1 Free Driving Mode

Free driving mode is one of the two modes considered in vehicles' longitudinal motion. When a vehicle keeps driving in a single lane, it is believed to be in Free driving mode if its space headway exceeds a threshold d(d=36.58m(120feet) from experience). In this mode, the driver usually hopes to control his vehicle speed on an expected value. The vehicle acceleration is supposed to satisfy

$$a(t+\tau) = \lambda(v^*(t) - v(t)) + \xi, \tag{17}$$

where τ is the driver's reaction time, $v^*(t)$ and $v(t)$ are the expected and actual velocities, λ is the sensitivity coefficient that reflects the driver's characteristics, ξ is a random number that is normally distributed.

Obviously, the vehicle's expected velocity $v^*(t)$ is restricted by traffic rules and road conditions. Moreover, it also depends on human's common driving experience. For example, the driver may choose a most comfortable velocity as $v^*(t)$ to reduce unnecessary driving operations and minimize driving burdens. Therefore, for the same road segment, the expected velocities of the same type of vehicles can be seen as the same, then the acceleration $a(t+\tau)$ is closely related to $v(t)$. As a result, in (12), when $\mathrm{DM}_\alpha^{(r-1)}$ is Free driving, the vehicle's velocity $v(t)$ is chosen to represent $\mathrm{MS}_\alpha^{(r-1)}$. Through analyzing Free driving trajectories extracted from the data set, the acceleration histograms under different driving velocities can be obtained. Fig. 6 shows the acceleration conditional PDs of automobiles in Free driving mode. The horizontal axis represents possible acceleration values $\{-3.66, -3.05, ..., 3.66\}\mathrm{m/s}^2(\{-12, -10, ..., 12\}\mathrm{feet/s}^2)$, while the vertical axis represents the corresponding probabilities.

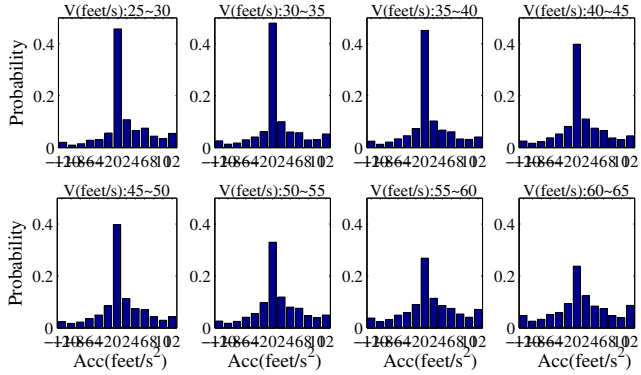

Fig. 6. Automobiles' acceleration conditional PDs given different diving velocities

From the above PDs, we can see that the probability of the acceleration $a = 0$ is far higher than the ones of a taking other values. The reason is that the vehicle acceleration usually does not change distinctly unless the drivers take concrete actions(i.e. throttle or braking). As a result, for most of the time, the drivers tend to maintain their current velocities. But as the velocities increase, the probabilities of $a = 0$ gradually decrease and the acceleration PD tends to be uniform. It is because that the driving decision-making processes become more complicated, and the uncertainties in trajectories become stronger.

In Free driving mode, (12) can be rewritten as

$$\begin{gathered} F_{\alpha a}^{(r)} \triangleq \left\{ q_{\alpha k}^{(r)}, k \in \{1, 2, ..., K\} \right\}, \\ q_{\alpha k}^{(r)} = P(a_\alpha^{(r)} = a_k | \mathrm{DM}_\alpha^{(r-1)} = \text{Free driving}, \\ \mathrm{MS}_\alpha^{(r-1)} = v_\alpha^{(r-1)}), \end{gathered} \tag{18}$$

where $v_\alpha^{(r-1)}$ is α's velocity at $t = (r-1)T$. With $F_{\alpha a}^{(r)}$ in (18), α's longitudinal probabilistic trajectory in Free driving mode can be computed with (11)(14).

4.2 Vehicle-Following Mode

Compared with Free driving mode, Vehicle-following mode is more common in urban traffic. A vehicle is thought to be in Vehicle-following mode if its space headway is less than d. Here the major factors that can influence a vehicle's acceleration are its space headway and relative velocity. According to the classical model in Gazis et al. (1959), the vehicle acceleration should satisfy

$$a(t+\tau) = \lambda \Delta v(t) / \Delta s(t)\ , \tag{19}$$

where $\Delta v(t)$ and $\Delta s(t)(\Delta s(t) > 0)$ are the relative velocity and space headway of the predicted vehicle, τ is the driver's reaction time. λ is the sensitivitv coefficient.

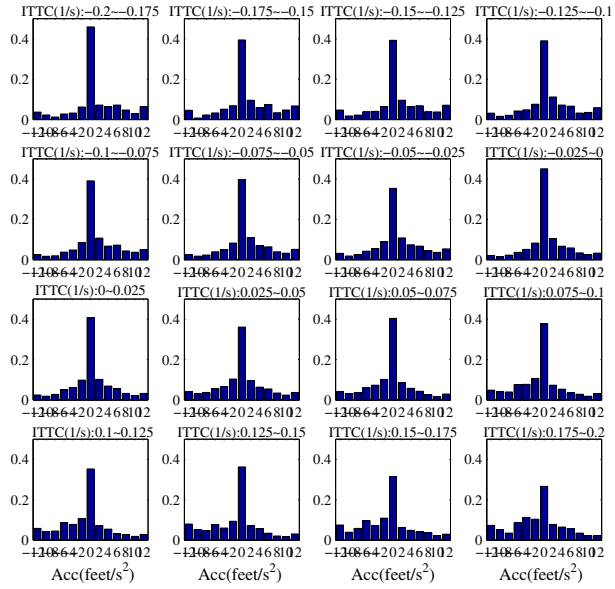

Fig. 7. Automobiles' acceleration conditional PDs given different ITTCs

Obviously, according to (19), the acceleration in Vehicle-following mode is closely related to $\Delta v(t)/\Delta s(t)$. Given that ITTC $= \Delta v(t)/\Delta s(t)$, then TTC(the inverse of ITTC, TTC $= \Delta s(t)/\Delta v(t)$) denotes the remaining time before the collision happens if both vehicles keep driving at their current velocities. As a result, the acceleration is closely related to ITTC. Thus in (12), when $\mathrm{DM}_\alpha^{(r-1)}$ is Vehicle-following, ITTC is chosen to represent $\mathrm{MS}_\alpha^{(r-1)}$. Through analyzing Vehicle-following trajectories extracted from the data set, the acceleration histograms under

different ITTCs can be obtained. Fig. 7 shows the acceleration conditional PDs of automobiles. The meaning of its coordinate axis is the same as defined in Fig. 6.

From the above PDs, when ITTC $\leq$ 0, the following vehicle is driving at a slower speed than the preceding one, so that it is more possible to accelerate, i.e. the probability of $a > 0$ is larger than the one of $a < 0$(see the top half of Fig. 7). Conversely, when ITTC $\geq$ 0, the vehicle is more possible to decelerate(see the bottom half of Fig. 7). In addition, it is noted that the probability of $a = 0$ decreases with the increase of ITTC. The reason is that the reaction time for taking actions to avoid collisions reduces with a higher ITTC. The drivers have to adjust their vehicle velocities more frequently to ensure safety.

When computing the motion state in the next moment, we need to know the acceleration conditional PD in the current moment. Different from Free driving mode, here $\mathrm{MS}_\alpha^{(r-1)}$(i.e. $\mathrm{ITTC}_\alpha^{(r-1)}$) needs to be computed with the space headway and relative velocity:

$$\mathrm{ITTC}_\alpha^{(r-1)} = \frac{v_\alpha^{(r-1)} - E(v_\beta^{(r-1)})}{E(s_\beta^{(r-1)}) - s_\alpha^{(r-1)}}, \tag{20}$$

where $E(s_\beta^{(r-1)})$ and $E(v_\beta^{(r-1)})$ are the expectations of the preceding vehicle β's longitudinal position and velocity at $t = (r-1)T$. In Vehicle-following mode, (12) can be rewritten as

$$\begin{gathered} F_{\alpha a}^{(r)} \triangleq \left\{ q_{\alpha k}^{(r)}, k \in \{1, 2, ..., K\} \right\}, \\ q_{\alpha k}^{(r)} = P(a_\alpha^{(r)} = a_k | \mathrm{DM}_\alpha^{(r-1)} = \text{Vehicle-following}, \\ \mathrm{MS}_\alpha^{(r-1)} = \mathrm{ITTC}_\alpha^{(r-1)}). \end{gathered} \tag{21}$$

With $F_{\alpha a}^{(r)}$ in (21), α's longitudinal probabilistic trajectory in Vehicle-following mode can be computed with (11)(14).

5. SIMULATION RESULTS

In this section, the proposed prediction model is demonstrated with numerical examples. The adopted data set is from *The US 101 Data Set* provided by the program NGSIM, which records vehicles' realtime trajectory data on a 2100-foot, six-lane highway segment. The recorded vehicle motion states include the relative(absolute) longitudinal and lateral positions, velocities, acceleration, space headway, time headway, etc. Trajectory data of three types of vehicles whose total length is 7500s, is extracted from the data set as model training data to identify model parameters. The PD parameters in the lateral motion model are lateral position PDs of different types of vehicles(see Fig. 5). The PD parameters in the longitudinal motion model are acceleration PDs in Free driving and Vehicle-following modes(the PDs of automobiles in two driving modes are shown in Fig. 6 and Fig. 7, respectively). The correction parameter is finally chosen as $\theta_{opt} = 0.07$. 53 automobiles' trajectory data(whose total length is 2000s) is applied to test and compare the performances of the proposed model and traditional model. All the simulations are executed in Visual Studio 2010 using a Intel(R) Core(TM) i5 CPU M 480@2.67GHz with RAM 2.0Gb. The algorithm parameters are shown in table 1.

Trajectory prediction is executed for 3 vehicles who drive on a two-lane road segment. The initial values of their motion parameters are shown in table 2. Fig. 8 demonstrates their position PDs at discrete moments. Pixels with different gray values are used to describe two-dimensional PDs, where the gray value is proportional to the possibility that there exist vehicle bodies(not the mass points that represent vehicles) in the corresponding region. Fig. 8(a),8(b),8(c) demonstrate the predicted position PDs of 3 vehicels at $t = 0$s, $t = 3$s and $t = 6$s, while Fig. 8(d) demonstrates the PDs at $t = 6$s if the interaction between vehicle trajectories is not considered. As is shown in Fig. 8(c), the prediction result reflects the trend that β decelerates because it is too close to γ. If the interaction between vehicle trajectories is not modeled, β will collide with γ with a high probability(see Fig. 8(d), β's position PD obviously overlaps with γ's).

Table 1. The values of algorithm parameters

Δw(feet)	L	Δs(feet)	I	s_I(feet)
1	12	0.5	800	400
T(s)	T_{pre}(s)	Δv(feet/s)	J	v_J(feet/s)
0.1	6	0.2	375	75

Table 2. The initial values of motion parameters

	Vehicle type	Driving lane	Velocity (feet/s^2)	Longitudinal position(feet)	Driving mode
α	Motor	A	30	20	Free driving
β	Auto	B	20	20	Vehicle-following
γ	Truck	B	15	90	Free driving

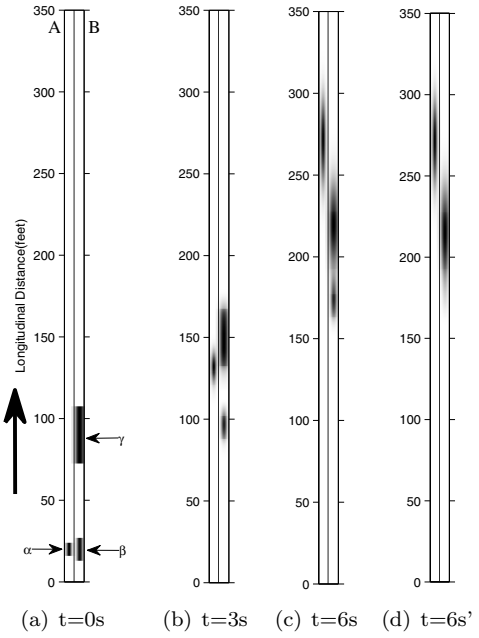

(a) t=0s (b) t=3s (c) t=6s (d) t=6s'

Fig. 8. Probabilistic trajectories in a multi-vehicle traffic scenario

Fig. 9 and Fig. 10 demonstrate the test results of model performance. The adopted variables are illustrated in table 3. Fig. 9 compares the influence of different algorithm parameters on the proposed Probabilistic Trajectory Model(PTM). Fig. 9(a) analyzes two PTMs with Δs = 0.15m(0.5feet) and Δs = 0.30m(1feet), and shows the relation between T_{cal} and T_{pre},Δs: $T_{cal} \propto T_{pre}^2/\Delta s$. The

reason is that, on one hand, the number of outer iterations for trajectory prediction I_{out} satisfies $I_{out} \propto T_{pre}$. On the other hand, when we compute the motion state PD in the next moment, we need to traverse all discrete states in the present moment. Consequently, the number of inner iterations I_{in} is proportional to the number of discrete states N_{state}. Furthermore, $N_{state} = I \cdot J$(I and J are the number of longitudinal position and velocity states), and I is usually chosen as $I = v_J \cdot T_{pre}/\Delta s$($v_J$ is the largest possible velocity), so that $I_{in} \propto T_{pre}/\Delta s$. Taken together, if we ignore other constant computation cost, $T_{pre} \propto I_{out} \cdot I_{in}$, so $T_{cal} \propto T_{pre}^2/\Delta s$. In order to meet the real-time requirement, PTM should ensure trajectory prediction for multiple vehicles are finished in T_{pre}. If we consider the ego vehicle's preceding and following vehicles, and 6 ones in the left and right neighbor lanes, we get 8 predicted objects. T_{cal} should satisfy

$$T_{pre}/T_{cal} > 8. \tag{22}$$

In Fig. 9(a), a group of algorithm parameters that make (T_{pre}, T_{cal}) falls below the dashed line can ensure that (22) works. Then PTM's real-time capability is guaranteed.

Fig. 9(b) analyzes PTM with $T_{pre} = 5$s and demonstrates the relative curves between Δs and its T_{cal},ERR$_{lon}$. From the discussion above, $T_{cal} \propto 1/\Delta s$, which is shown by the star line in Fig. 9(b). The dotted line shows how ERR$_{lon}$ changes over Δs. Note that, when $\Delta s < 0.15$m(0.5feet), with the decreasing of Δs, T_{cal} increases rapidly but ERR$_{lon}$ goes down slowly. Therefore, Δs is a critical algorithm parameter that need to be designed based on the prediction accuracy requirement and application environment. A balance between prediction error and computing time is required.

Table 3. The illustration of variables used in model performance tests

Δs	The length of longitudinal position intervals
T_{pre}	Trajectory prediction time horizon
T_{cal}	The time consumed for calculating a probabilistic trajectory
ERR$_{lat}$	Average largest prediction error of lateral positions
ERR$_{lon}$	Average largest prediction error of longitudinal positions

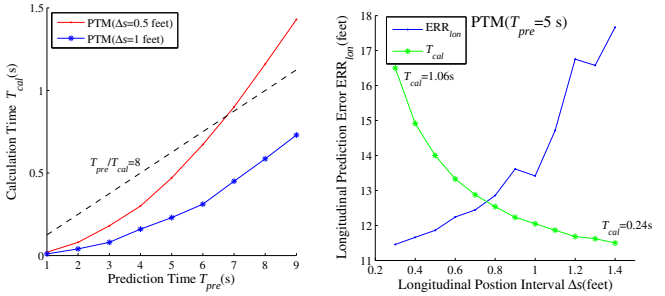

(a) The relation curves between T_{cal} and T_{pre} (b) The relation curves between ERR$_{lon}$, T_{cal} and Δ_s

Fig. 9. The influence of algorithm parameters on PTM performance

Fig. 10 analyzes two PTMs with $\Delta s = 0.15$m(0.5feet) and $\Delta s = 0.30$m(1feet), and compares the prediction error of PTMs with Constant Velocity Model(CVM). CVM is usually applied in traditional methods to make prediction, which simply assumes that vehicles keep driving at constant speeds along the lane centerlines. As is shown in Fig. 10, there is no remarkable distinction between ERR$_{lat}$ of PTM and CVM. Also, their ERR$_{lon}$ both go up with the increasing of T_{pre}. But when $T_{pre} \geq 2$s, the ERR$_{lon}$ of PTM(Δs=0.5feet) is less than the one of CVM, and PTM performs better with a higher T_{pre}. It is because that the changes of vehicle velocities are not obvious in a short time, so the assumption of constant velocities is acceptable. But as time goes on, the effect of driving decisions will accumulate, which may result in a significant increase of CVM's prediction error. For PTMs, since they consider the update of acceleration PDs with the changing environment, more accurate prediction results can be acquired.

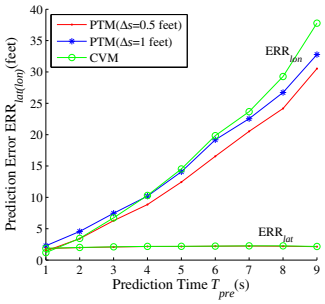

Fig. 10. The prediction error comparison of PTM with CVM

According to the above analysis, PTM can provide a better prediction than CVM and can meet the real-time requirement. When applying PTM in intelligent driving, for convenience, we can directly use the expectations of vehicle position PDs as the deterministic prediction results. Furthermore, in order to make fully use of the probability information, we can define the influence of α's future trajectory on the ego vehicle as

$$J_\alpha \triangleq \sum_{l,i,r} p_{\alpha l}^{(r)} p_{\alpha i}^{(r)} \cdot I(l,i,r), \tag{23}$$

where $I(l,i,r)$ is the evaluation of α's influence on the ego vehicle at $t = rT$ if α is in the rectangular region $W_l \cap S_i$.

6. CONCLUSION

Without considering the uncertainties in vehicle driving, traditional trajectory prediction methods can only provide unique deterministic results. They do not consider the complexity of real driving behaviors. To solve this problem, based on the work in Althoff et al. (2009), we propose a novel probabilistic method to make prediction for single lane driving trajectories. In our model, the possibilities of different trajectory executions(i.e. probabilistic trajectories) are described as vehicles' position PDs at different time points. In order to simulate driving behaviors more realistically, this model also considers the characteristics of different types of vehicles, and the interaction between vehicle trajectories. Model parameters are identified off-line based on historical trajectory data, thus on-line computation burden is greatly reduced. The simulation results show that, the proposed model can be applied in real-time and its prediction error is less than the traditional

model. This method is suitable for driving assistance systems and autonomous vehicles, which can be applied in driving decision-making, trajectory planning, and collision warning.

Lane changing is a more complex driving behavior on urban roads. Their driving decision-making processes are more complicated than single lane driving, thus the uncertainty of their trajectories is more serious. Based on the proposed model here, the prediction of lane changing trajectories will be researched in future work.

REFERENCES

Althoff, M., Stursberg, O., and Buss, M. (2009). Model-based probabilistic collision detection in autonomous driving. *Intelligent Transportation Systems, IEEE Transactions on*, 10(2), 299–310.

Broadhurst, A., Baker, S., and Kanade, T. (2005). Monte carlo road safety reasoning. In *Intelligent Vehicles Symposium, 2005. Proceedings. IEEE*, 319–324. IEEE.

Danielsson, S., Petersson, L., and Eidehall, A. (2007). Monte carlo based threat assessment: Analysis and improvements. In *Intelligent Vehicles Symposium, 2007 IEEE*, 233–238. IEEE.

Ferguson, D., Darms, M., Urmson, C., and Kolski, S. (2008). Detection, prediction, and avoidance of dynamic obstacles in urban environments. In *Intelligent Vehicles Symposium, 2008 IEEE*, 1149–1154. IEEE.

Gazis, D.C., Herman, R., and Potts, R.B. (1959). Car-following theory of steady-state traffic flow. *Operations Research*, 7(4), 499–505.

Glaser, S., Vanholme, B., Mammar, S., Gruyer, D., and Nouveliere, L. (2010). Maneuver-based trajectory planning for highly autonomous vehicles on real road with traffic and driver interaction. *Intelligent Transportation Systems, IEEE Transactions on*, 11(3), 589–606.

Jula, H., Kosmatopoulos, E.B., and Ioannou, P.A. (2000). Collision avoidance analysis for lane changing and merging. *Vehicular Technology, IEEE Transactions on*, 49(6), 2295–2308.

Kammel, S., Ziegler, J., Pitzer, B., Werling, M., Gindele, T., Jagzent, D., Schröder, J., Thuy, M., Goebl, M., Hundelshausen, F.v., et al. (2008). Team annieway's autonomous system for the 2007 darpa urban challenge. *Journal of Field Robotics*, 25(9), 615–639.

Keller, C.G., Dang, T., Fritz, H., Joos, A., Rabe, C., and Gavrila, D.M. (2011). Active pedestrian safety by automatic braking and evasive steering. *Intelligent Transportation Systems, IEEE Transactions on*, 12(4), 1292–1304.

Krumm, J. (2008). A markov model for driver turn prediction. *SAE SP*, 2193(1).

Labayrade, R., Royere, C., and Aubert, D. (2005). A collision mitigation system using laser scanner and stereovision fusion and its assessment. In *Intelligent Vehicles Symposium, 2005. Proceedings. IEEE*, 441–446. IEEE.

Pentland, A. and Liu, A. (1999). Modeling and prediction of human behavior. *Neural computation*, 11(1), 229–242.